INVESTIGATION OF THE PHOTOCATALYTIC PROPERTIES OF Er^{3+} AND Yb^{3+} DOPED STRONTIUM GADOLINIUM OXIDE NANOPOWDER

Tijana Stamenković[1], Marjan Ranđelović[2], Vesna Lojpur[1]*

[1]Laboratory for Atomic Physics, "Vinča" Institute of Nuclear Sciences, National Institute of the Republic of Serbia, University of Belgrade, Belgrade, Serbia
[2]Department of Chemistry, Faculty of Science and Mathematics, University of Niš, Niš, Serbia

(ORIGINAL SCIENTIFIC PAPER)
UDC: 544.526.5:546.42'662
DOI: 10.5937/savteh2302004S

This research aimed to investigate for the first-time photocatalytic degradation of methylene blue over $SrGd_2O_4$ powders co-doped with constant Er^{3+} (0.5 at%) and different Yb^{3+} (1, 2.5 and 5 at%) concentrations. The samples were successfully prepared via sol-gel assisted combustion method. X-ray Powder Diffraction pattern proved that all samples crystallize as a pure orthorhombic $SrGd_2O_4$ phase. Scanning Electron Microscopy was used for morphology characterization and it revealed the existence of porous agglomerated round-shaped particles. Energy Dispersive X-ray Spectroscopy showed the presence of dopant ions and even distribution of all constituting elements. For energy band calculation, UV-VIS Diffuse Reflectance Spectroscopy was performed and a value of 4.3 eV was obtained, as well as the four additional values from the bands at lower energies. Photocatalytic degradation of methylene blue was monitored using UV-VIS Absorption Spectroscopy. The obtained results were promising since after 4 h of exposure to the simulating Sun irradiation, more than 50% of the starting dye concentration was mineralized.

Keywords: Photocatalysis, luminescence, rare earth, up-conversion, water purification

Introduction

Environmental pollution stands for one of the most imperative topics in modern society. Many different methods for air and water purification exist nowadays and even more are currently in the developing process. One of them is photocatalysis, widely explored especially for water treatments, with promising results so far. The idea is to use sunlight to mineralize pollutants utilizing particular photocatalysts down to non-toxic molecules such as CO_2 and H_2O. Semiconductors, mostly oxides, are mainly used as photocatalysts because of their desirable characteristics and affordability [1].

To further exploit the energy of the Sun, various approaches have been developed to improve photocatalysts' properties, for example, doping with different elements. Some anticipated properties can be obtained by doping with rare earth (RE) elements [2]. These elements can alter or even promote other material characteristics, such as photoluminescence (PL). Luminescent materials have an extensive range of potential for many different applications (medicine, industry, environmental, etc.). Their visible light emission is caused by the existence of abundant energy levels which originate from the RE elements. Depending on the chosen RE to be used as the luminescent center, as well as the selected host matrix, emitted light with precisely tuned colors can be obtained. The choice of dopant RE ions also determines whether the luminescent material will be down- or up-converting. [3].

One of the combinations that have shown great potential for producing efficient up-convertors includes Er^{3+} and Yb^{3+}. In these systems, Er^{3+} ions act as activators since they provide visible light emission, while Yb^{3+} ions are utilized to absorb infrared (IR) radiation [4–6]. A combination of these two elements incorporated in various hosts, but mostly in diverse composites, has been studied for application in photocatalysis [7–10]. Since up-conversion increases absorption in the near-IR (NIR) region, which includes around 40% of the Solar irradiation, theoretically, that may enhance the photocatalytic activity of the material by boosting charge separation [11]. This opportunity enables harvesting a wider range of solar spectrum and using more of this clean and abundant energy.

Our previously published paper regarding Er^{3+} and Yb^{3+} doped $SrGd_2O_4$ host showed different characterization techniques, luminescent properties and quantum yield inspection [12]. To the best of our knowledge, there is no information in the literature regarding the investigation of the photocatalytic properties of the $SrGd_2O_4$:Er,Yb system. The goal of this research is to examine other

*Author address: Vesna Lojpur, Laboratory for Atomic Physics, "Vinča" Institute of Nuclear Sciences, National Institute of the Republic of Serbia, University of Belgrade, Belgrade, Serbia;
e-mail address: lojpur@vin.bg.ac.rs
The manuscript received: April, 13, 2023.
Paper accepted: August, 15, 2023.

characteristics of as-synthesized nanoparticles and perform test reactions to examine their potential application as photocatalysts for the mineralization of methylene blue (MB) as a model pollutant.

Experimental

Materials

For the sample preparation as well as the photocatalysis, the subsequent materials were used: glycine, citric acid (Kemika 99.5% and 99.0%, respectively), $Sr(NO_3)_3$ (Puratonic, 99.9%), $Gd(NO_3)_3*6H_2O$, $Er(NO_3)_3*5H_2O$ (Acros Organics, 99.9%), $Yb(NO_3)_3*5H_2O$ (Sigma Aldrich, 99.9%) and methylene blue (Fisher chemicals) were used without further purification.

Synthesis

The samples of $SrGd_2O_4$ nanopowders doped with a constant concentration of Er^{3+} (0.5 at%) and different concentrations of Yb^{3+} (1, 2.5 and 5 at%) were made with citric acid (chelator) and glycine (fuel). The preparation procedure was described in detail in our recent publication [12]. Solutions of Gd^{3+}, Er^{3+} and Yb^{3+} or Sr^{2+} were created by dissolving the required amounts of nitrates in deionized water. After citric acid was mixed with the solutions, the temperature was elevated to 70 °C. Next, both solutions were merged, glycine was added, and the temperature was elevated to 120 °C. Mixing was continued until a wet gel was formed which was then thermally treated for 1.5 hours at 500 °C. Finally, the calcination was conducted for 2.5 hours at 1000 °C and white nanopowder was obtained.

Characterization techniques

To inspect the phase purity and crystallinity of the as-synthesized powders, X-ray powder diffraction (XRPD) was utilized (Rigaku Ultima IV, Japan). The used X-ray beam was nickel-filtered CuKα1 radiation (λ = 0.1540 nm, running at 40 mA and 40 kV). The scanning rate was 2°/min and the information data were gathered from 10 to 70° (2θ).

Morphology and particle size were investigated by using Field emission scanning electron microscopy (FESEM - FEI Scios 2, the operating voltage of 30 kV), whilst the presence and arrangement of chemical elements were observed by using energy-dispersive X-ray spectroscopy (EDS).

UV-VIS spectra were acquired with a UV-2600I spectrophotometer (Shimadzu, with an integrated sphere attachment). Absorbance spectra for the study of the photocatalytic decomposition of MB were collected in the range from 200 to 800 nm. Diffuse reflectance spectroscopy (DRS) was performed in the range of 200 to 1200 nm and energy gap (Eg) values of as-synthesized nanopowders were obtained by using the Kubelka-Munk function.

Photocatalytic test

Photocatalytic decomposition of MB was conducted in an aqueous solution onto as-synthesized $SrGd_2O_4$ nanopowders doped with Er^{3+} and Yb^{3+} under simulated Sun illumination. A certain amount of catalyst (10 or 20 mg) was loaded in a glass filled with 50 ml of MB solution (1, 3, 5 or 10 ppm). First, the reaction solution remained in the dark for 60 minutes prior to illumination to achieve an adsorption-desorption balance. Then, the system was irradiated by the lamp (Osram Vitalux lamp, 300 W, Sunlight simulation, white light: UVB radiated power from 280 to 315 nm, 3.0 W, UVA radiated power 315–400 nm 13.6 W; the rest is visible light and IR) positioned 30 cm directly over the dye solution. The reaction solution was constantly cooled at 15±1 °C to avoid heating and/or evaporation. Also, the constant flow (1.5 dm^3/min) of O_2 in the MB solution was enabled. At proper time intervals, aliquots were drawn for the analysis. After the centrifugation for altogether 30 minutes (3 times at 8000 rpm for 10 minutes), the UV-VIS absorption spectra of each aliquot were recorded. To ensure the even dispersal of the catalyst particles in the system, the solution was placed on the magnetic stirrer with constant rotation speed.

Results and discussion

It is already declared that our previous paper [12] concerning $SrGd_2O_4$ doped with Er^{3+} and Yb^{3+} studied its luminescent properties, therefore, only important facts related to luminescence will be mentioned in this paper. The PL emission spectra of this up-converting phosphorus revealed peaks assigned to the trivalent erbium f-f electronic transitions: one red emission at 661 nm due to $^4F_{9/2} \rightarrow {}^4I_{15/2}$ transition and two green emissions at 551 and 523 nm from $^4S_{3/2} \rightarrow {}^4I_{15/2}$ and $^2H_{11/2} \rightarrow {}^4I_{15/2}$ transitions. The sample containing the highest concentration of Yb^{3+} (5 at%) displayed the most intensive emission. For this reason, a sample with 5 at% of Yb was chosen to be examined in the photocatalytic application for the decomposition of organic dye MB.

X-ray Powder Diffraction

XRPD measurements were performed to examine the structural characteristics of this newly synthesized material. All three samples confirmed identical diffractograms, but only one of the $SrGd_2O_4$ doped with the highest content of Yb^{3+} (5%) as representative is presented in Figure 1. The crystallinity and phase purity of the obtained powders revealed that samples are monophase since all diffraction peaks are well indexed to the orthorhombic lattice $SrGd_2O_4$ (space group *Pnma*). There are no additional peaks that indicate the formation of another phase or some other impurity, which implies that introducing dopant ions did not affect or change the original crystal structure of $SrGd_2O_4$.

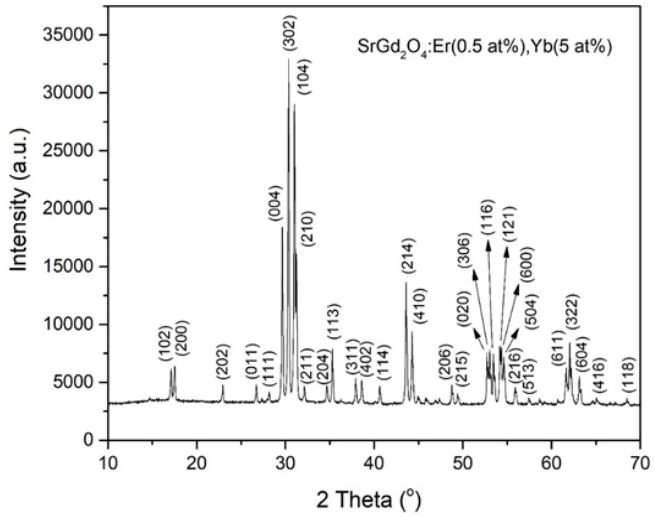

Figure 1. XRPD diffractogram of the $SrGd_2O_4$:Er,Yb (5 at% Yb^{3+})

Field Emission Scanning Electron Microscopy

The morphology and chemical composition of the samples were provided using SEM and EDS analysis. Figure 2. reveals EDS spectrum and FESEM images of the $SrGd_2O_4$:Er,Yb (5 at% Yb^{3+}) at different magnifications as insets (a and b). EDS investigation confirmed the existence of the composing elements (Sr, Gd, O) as well as of the dopants (Er and Yb). Additionally, SEM micrographs discovered agglomerated but porous structures, composed of tightly crowded round-shaped particles. The existence of smaller particles which are less than 50 nm in diameter is also observed. The pores have different shapes and dimensions which vary from 50 nm up to a few hundred nm. These morphological properties are probably a direct consequence of the preparation method since a large quantity of produced gasses during synthesis may incite the appearance of holes and voids in the material. Accordingly, considering the dimension of the MB molecule [13], it could be expected that the morphology of this sample will be suitable for the photocatalytic reaction of the selected dye.

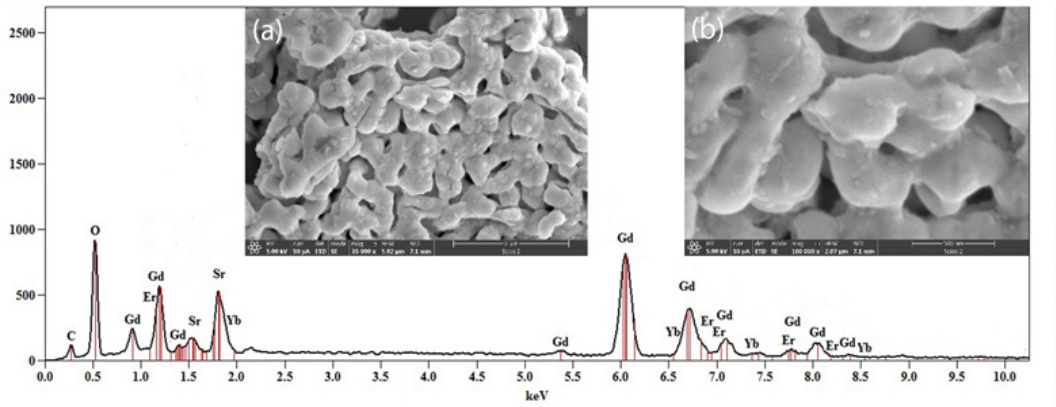

Figure 2. EDS spectrum and FESEM images of the $SrGd_2O_4$:Er,Yb (5 at% Yb^{3+}) at different magnifications as insets (a, b)

UV-VIS Diffuse Reflectance Spectroscopy

DRS measurements were completed in order to obtain the information on optical band gap energy of the material. The results for the sample with 5 at% of Yb^{3+} are presented in Figure 3. The reflectance spectrum (Figure 3a) demonstrates peaks that correspond to the transition states that originate mostly from Er^{3+} ions, but also that of Gd^{3+} at lower (below 300 nm) and Yb^{3+} at higher (above 900 nm) wavelengths [14–16]. The appearance of these peaks also illustrates another method to verify the chemical composition and confirms the efficacious doping of Er^{3+} and Yb^{3+} ions. Furthermore, the Kubelka-Munk function in the form of the direct allowed transition was used in order to estimate Eg value (Figure 3b). The band gap approximation was done by linear extrapolation of the adsorption edge to the energy axis from the calculated *F*(*R)* (Eq. 1.):

$$F(R) = \frac{(1-R)^2}{2R} \quad \text{.....(1)}$$

where *R* is the diffuse reflectance of the investigated sample. The obtained Eg value was found to be 4.3 eV, with four additional values from lower energy band levels at 2.2 eV, 2.7 eV, 3.1 eV and 3.7 eV. As reported in our previous paper [15], Eg values for the un-doped $SrGd_2O_4$ were 2.7 eV, 3.7 eV and 4.3 eV, which all appear to be observable in $SrGd_2O_4$:Er,Yb sample as well. Additional energies are indicators that oxygen vacancies or other defects are integrated into the matrix to form extra energy states in the energy gap that could potentially have a positive effect on the following photocatalytic degradation process. In this case, the incorporation of the Er^{3+} and Yb^{3+} ions in the $SrGd_2O_4$ crystal lattice creates intermediate energy states (2.2 eV and 3.1 eV) which are positioned below the conduction band. Moreover, the lowest energy gap at 2.2 eV corresponds to a wavelength of around 563 nm which belongs to the visible part of the Solar spectrum. Since the light source used for the photocatalytic experiment simulate Solar irradiation, the above stated fact represents an advantage for better

light utilization and improved photocatalytic degradation of MB.

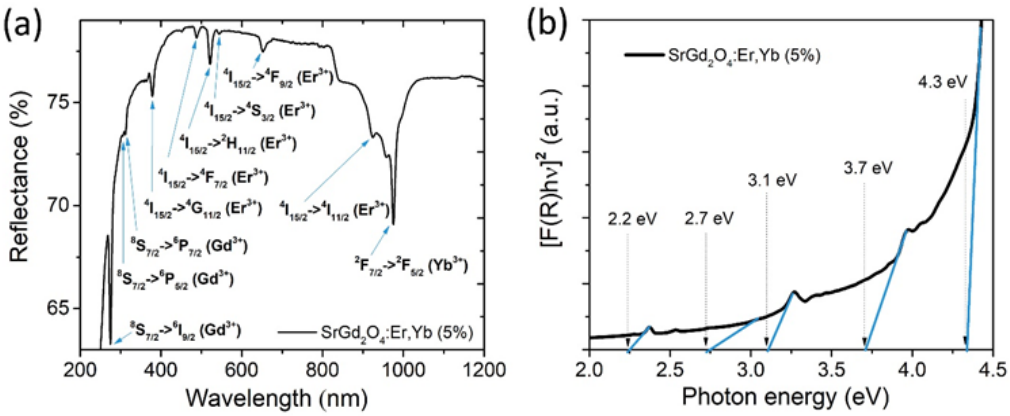

Figure 3. DR spectrum (a) and Kubelka-Munk plot (b) for $SrGd_2O_4$:Er,Yb (5 at% Yb^{3+})

Photocatalytic experiment

A well-known fact is that photocatalysis stands for one of the most imperative applications for wastewater treatments. The photocatalytic mechanism proposes the creation of the highly reactive species ($O_2^{-\bullet}$, OH•, H_2O_2) due to light exposure in the reactions between the photogenerated electrons and holes on one side, and adsorbed oxygen and water molecules on the other. These species further participate in the degradation of the selected pollutant until that molecule is ultimately decomposed to the non-toxic compounds, such as CO_2, H_2O, or some inorganic anion [13,17].

The degradation mechanism of cationic dye MB has been extensively studied [13,18,19]. The absorption peak of the MB monomer reaches maximum intensity at 664 nm, while a less intensive peak at 614 nm is ascribed to MB dimer. Another two peaks at 292 nm and 246 nm are related to substituted benzene rings. As the photodegradation proceeds, the intensity of these peaks progressively decreases. If both peaks positioned above 600 nm decrease over time equivalently, it means that direct degradation of the dye by $OH^{\bullet}$ occurs. However, if there is a noticeable hypsochromic shift in the absorption spectra, then it is the case of step-by-step demethylation.

To explore the mechanism of the photocatalytic degradation of MB over $SrGd_2O_4$:Er,Yb, the results of the conducted experiments are presented in Figure 4. The influence of the processing parameters such as MB concentration (Figure 4a) and catalyst mass (Figure 4b) on the degradation rate was investigated. Since UV-VIS absorption spectra demonstrated similar spectral changes for every photocatalytic reaction, the authors chose to present only one for the reaction where 3 ppm MB and 10 mg of the catalyst were used (Figure 4c). The absorption spectra clearly illustrate a similar reduction in peak intensity for both monomer and dimer MB. This suggests the reaction mechanism through direct degradation of the dye with $OH^{\bullet}$ as the dominant reactive species. It should be stressed that $OH^{\bullet}$ can also form from oxygen species, thus explaining favorable mechanisms via direct and complete degradation by hydroxyl radicals.

Moreover, if we discuss the possibility of the creation of the reactive species, radical generation potential must be compared to the band edge potential of the catalyst [20]. From the gathered UV-VIS DRS results and by using the proper empirical equations [15], we were able to calculate the conduction band (CB) and valence band (VB) potential (ECB and EVB, respectively) for $SrGd_2O_4$ doped with 0.5 at% Er^{3+} and 5 at% Yb^{3+}. The obtained value for ECB band edge potential is at -1.5 eV, and as for EVB band edge potential it is at +2.8 eV. Having in mind that radical generation potential for all important pairs ($O_{2\ ads}/O_2^{-\bullet}$ (-0.33 V, NHE), $OH^-_{ads}/OH^{\bullet}$ (+1.9 V, NHE) and $H_2O_{ads}/OH^{\bullet}$ (+2.32 V, NHE) [21]) are placed at the proper positions comparing to catalysts' band edge potential, it is presumable that all reactive species can be created in this system. It should be emphasized that MB/MB* potential [18] is also positioned adequately compared to catalyst band edge potential, hence, adsorbed dye on the catalyst particles can participate in charge transfer as well.

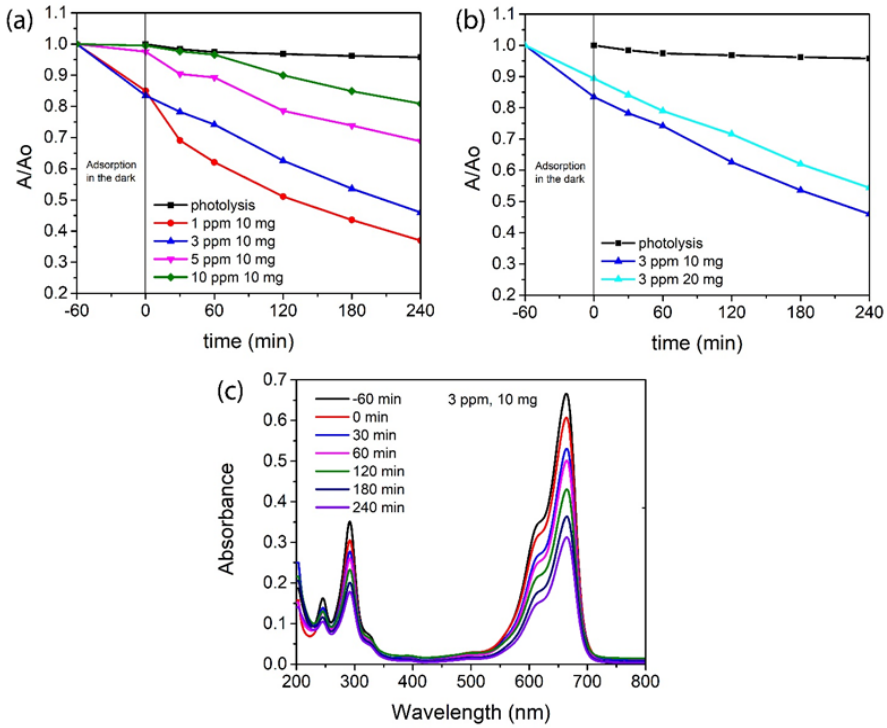

Figure 4. Kinetic curves of photolysis and photocatalysis of MB over $SrGd_2O_4$:Er,Yb (5 at% Yb^{3+}) for different BM concentrations (a), different catalyst mass (b) and UV-VIS degradation spectrum for reaction with 3 ppm MB and 10 mg catalyst (c)

Influence of initial MB concentration

The influence of different initial MB concentrations (1, 3, 5 and 10 ppm) on the photocatalytic degradation was examined, and degradation rates are presented in Figure 4a. First, it should be mentioned that reactions with lower dye concentrations have better adsorption onto the catalyst surface. Determination of the amount of MB adsorbed by the as-synthesized powder (adsorbent) at equilibrium condition was done by using the following equation (Eq. 2.) [18]:

$$q_e = \frac{(C_0 - C_e)}{m} x V \quad \text{.....(2)}$$

where q_e is the amount of MB adsorbed at equilibrium (mmol/g), C_0 and C_e symbolize the concentration of MB in the solution at initial and equilibrium condition, respectively, V (dm^3) is the volume of dye solution and m is the mass of catalyst (g). It was calculated that the amount of MB adsorbed onto the catalyst surface is 0.0072, 0.024, 0.0096 and 0.00339 mmol/g for dye concentrations of 1, 3, 5 and 10 ppm, respectively. The adsorption capacity rises until 3 ppm where it reaches the maximum. Additional increasing of the MB concentration leads to declining in adsorption capacity. Considering further drop of the MB concentration after exposure to light source, it can be seen that with a decrease in dye concentration from 10 ppm to 1 ppm, the degradation rate increases. By the end of the photocatalytic process, the best decomposition is achieved with the lowest MB concentration. Diminished MB degradation at higher concentrations is probably because of the reduced photon penetration to the catalyst surface due to the increased optical density of the solution [22]. This can also be explained by the „covering“ effect: the number of active sites on the catalyst is reduced as a result of the excessive dye adsorption, therefore, the creation of the reactive species is suppressed [23].

Influence of catalyst dosage

The effect of different catalyst masses (10 and 20 g) on the photocatalytic process was investigated and results are presented in Figure 4b. It can be observed that having more catalytic material in the system does not necessarily suggest better photocatalytic efficacy. Catalyst overloading may provoke the light scattering phenomenon and screening effect where penetration of light is hindered due to the excessive opacity of the reaction solution, hence, the photocatalytic ability is reduced. Enlarged aggregation can act as a light barrier and therefore prevent photons from reaching the surface which also lowers catalysts' specific activity [24].

Conclusion

$SrGd_2O_4$ nanopowders co-doped with Er^{3+} and Yb^{3+} ions were synthesized via sol-gel assisted combustion method. It was a challenge to inspect the photocatalytic

properties of this luminescent material in the process of MB degradation under simulated Sun irradiation since it has never been done before. XRPD diffractogram verified crystallization of as-synthesized samples as pure $SrGd_2O_4$ orthorhombic phase corresponding to space group *Pnma* and without any other impurities. Morphology was investigated using SEM and it was discovered that these samples consist of porous agglomerated round-shaped elements, with the smallest observed particles which are less than 50 nm in diameter. Elemental composition was examined with EDS, which confirmed the existence of all founding elements as well as the dopants, and their uniform distribution across the grains. UV-VIS measurements enabled calculation of the band gap energy which was determined at 4.3 eV, but also that of the four additional levels at 3.7 eV, 3.1 eV, 2.7 eV, and 2.2 eV. Photocatalytic degradation of methylene blue was studied as a possible application for this newly synthesized material. Even though it possesses luminescent capabilities (which are considered to be the opposite to the photocatalytic abilities, that suppress one another) the sample showed promising results regarding visible light driven photocatalysis. Monitored degradation reactions considered 4 h of exposure to the simulating Sun irradiation after which up to 60% of the starting MB concentration was mineralized. The influence of the MB concentration and catalyst dosage on the photocatalytic process was examined and results indicate that lower dye concentrations provide faster mineralization, as well as reduced catalyst dosage. The proposed reaction mechanism suggests direct and complete degradation of MB to non-toxic smaller fragments after longer period of time, or by optimizing process parameters.

Acknowledgments

The research was funded by the Ministry of Science, Technological Development and Innovation of the Republic of Serbia on the research program Grant No. 451-03-47/2023-01/ 200017 Vinča Institute of Nuclear Sciences.

References

[1] Ren G, Han H, Wang Y, Liu S, Zhao J, Meng X, Li Z. Recent advances of photocatalytic application in water treatment: *A review. Nanomaterials*. 2021, 11, 1804-1826. https://doi.org/10.3390/nano11071804

[2] Weber AS, Grady AM, Koodali RT. Lanthanide modified semiconductor photocatalysts. *Catalysis Science and Technology.* 2012, 2, 683–693. https://doi.org/10.1039/c2cy00552b

[3] Kitai A. *Luminescent materials and applications,* John Wiley & Sons, 2008. ISBN: 978-0-470-05818-3

[4] Nannuri SH, Samal AR, Subash CK, Santhosh C, George SD. Tuning of structural, laser power-dependent and temperature dependent luminescence properties of $NaYF_4$:Yb,Er (Y: 88%, Yb: 10 and Er: 2%) submicron crystals using Cr^{3+} ion doping. *Journal of Alloys and Compounds.* 2019, 777 894–901. https://doi.org/10.1016/j.jallcom.2018.11.035

[5] Liu W, Li Y, Song Y, Zhou X, Zheng K, Sheng Y, Shi Z, Zou H. Facile synthesis and multicolor luminescence properties of $Gd_4O_3F_6$:Ln^{3+} (Ln = Eu, Tb, Dy, Sm, Ho, Tm, Yb/Er, Yb/Ho) microcrystals. *Optical Materials.* 2019, 94, 92–102. https://doi.org/10.1016/j.optmat.2019.05.013

[6] Wang Y, Wen Z, Ye W, Feng Z, Zhao C, Zuo C, Li Y, Cao Z, Cao Z, Ma C, Cao Y. Enhanced green up-conversion luminescence in In_2O_3:Yb^{3+}/Er^{3+} by tri-doping Zn^{2+}. *Journal of Luminescence.* 2020, 221, 117029-117036. https://doi.org/10.1016/j.jlumin.2020.117029

[7] Regmi C, Kshetri YK, Ray SK, Pandey RP, Lee SW. Utilization of visible to NIR light energy by Yb^{+3}, Er^{+3} and Tm^{+3} doped $BiVO_4$ for the photocatalytic degradation of methylene blue. *Applied Surface Science*. 2017, 392, 61–70. https://doi.org/10.1016/j.apsusc.2016.09.024

[8] Li X, Li W, Liu X, Geng L, Fan H, Khan A, Ma X, Dong M, Qiu H. The construction of Yb/Er/Pr triple-doped Bi_2WO_6 superior photocatalyst and the regulation of superoxide and hydroxyl radicals. *Applied Surface Science*. 2022, 592, 153311-153321. https://doi.org/10.1016/j.apsusc.2022.153311

[9] Pickering JW, Bhethanabotla VR, Kuhn JN. Assessment of mechanisms for enhanced performance of TiO_2/YAG:Yb^{+3},Er^{+3} composite photocatalysts for organic degradation. *Applied Catalysis B: Environmental.* 2017, 202, 147–155. https://doi.org/10.1016/j.apcatb.2016.09.007

[10] Cruz-Puerto J, Ramirez-Carrillo C, Puga-Lechuga J, de la Mora P, Tavizon G. Crystal structure and optical absorption properties of Er and Yb doped $InTaO_4$ and $InTaO_4$-yNy as photocatalysts under visible light. *Chemical Physics Letters.* 2020, 739, 136998-137009. https://doi.org/10.1016/j.cplett.2019.136998

[11] Bhethanabotla VC, Russell DR, Kuhn JN. Assessment of mechanisms for enhanced performance of Yb/Er/titania photocatalysts for organic degradation: Role of rare earth elements in the titania phase. *Applied Catalysis B: Environmental.* 2017, 202, 156–164. https://doi.org/10.1016/j.apcatb.2016.09.008

[12] Stamenković T, Radmilović N, Prekajski Đorđević M, Rabasović M, Dinić I, Tomić M, Lojpur V, Mančić L. Quantum yield and energy transfer in up-conversion $SrGd_2O_4$:Yb,Er nanoparticles obtained via sol-gel assisted combustion. *Journal of Luminescence*. 2023, 253, 1–8. https://doi.org/10.1016/j.jlumin.2022.119491

[13] Khan I, Saeed K, Zekker I, Zhang B, Hendi AH, Ahmad A, Ahmad S, Zada N, Ahmad H, Ali Shah L, Shah T, Khan I. Review on Methylene Blue: Its Properties, Uses, Toxicity and Photodegradation. *Water.* 2022, 14, 422-452. https://doi.org/10.5040/9781501365072.12105

[14] Stamenković T, Radmilović N, Nikolić M, Erčić J, Lojpur V. Structural and Luminescence Properties of $SrGd_2O_4$ Nanocrystalline Phosphor Doped with Dy^{3+} and Sm^{3+}. *Science of Sintering.* 2022, 54, 295–303. https://doi.org/10.2298/SOS2203295S

[15] Stamenković T, Pjević D, Krstić J, Popović M, Rajić V, Lojpur V. Characterization and photocatalytic application of $SrGd_2O_4$ doped with rare earth Sm^{3+} and Dy^{3+} ions. *Surfaces and Interfaces*. 2023, 37, 102755-102757. https://doi.org/10.1016/j.surfin.2023.102755

[16] Wang Y, Zuo C, Ma C, Ye W, Zhao C, Feng Z, Li Y, Wen Z, Wang C, Shen X, Yuan X, Cao Y. Effects of Sc^{3+} ions on

local crystal structure and up-conversion luminescence of layered perovskite NaYTiO4: Yb^{3+}/Er^{3+}. *Journal of Alloys and Compounds*. 2021, 876, 160166-160175. https://doi.org/10.1016/j.jallcom.2021.160166
[17] Wojcieszak D, Kaczmarek D, Domaradzki J, Mazur M. Correlation of photocatalysis and photoluminescence effect in relation to the surface properties of TiO_2:Tb thin films. *International Journal of Photoenergy.* 2013, 2013, 1-9. https://doi.org/10.1155/2013/526140
[18] Savić TD, Carević MV, Mitrić MN, Kuljanin-Jakovljević J, Abazović ND, Čomor MI. Simulated solar light driven performance of nanosized $ZnIn_2S_4$/dye system: decolourization vs. photodegradation. *Journal of Photochemistry and Photobiology A: Chemistry*. 2020, 388, 112154-112163. https://doi.org/10.1016/j.jphotochem.2019.112154
[19] Houas A, Lachheb H, Ksibi M, Elaloui E, Guillard C, Herrmann JM. Photocatalytic degradation pathway of methylene blue in water. *Applied Catalysis B: Environmental.* 2021, 31, 145–157. https://doi.org/10.1016/S0926-3373(00)00276-9
[20] Fujishima A, Zhang X, Tryk DA. TiO_2 photocatalysis and related surface phenomena. *Surface Science Reports.* 2008, 63, 515–582. https://doi.org/10.1016/j.surfrep.2008.10.001
[21] Vulić TD, Carević MV, Abazović ND, Novaković TB, Mojović ZD, Čomor MI. Application of Zirconia/Alumina Composite Oxide Ceramics as Photocatalysts for Removal of 2,4,6-Trichlorophenol from Water. *Photochem.* 2022, 2, 905–917. https://doi.org/10.3390/photochem2040058
[22] Vasić MB, Randjelović MS, Momčilović MZ, Matović BZ, Zarubica AR. Degradation of crystal violet over heterogeneous TiO_2-based catalysts: The effect of process parameters. *Processing and Application of Ceramics*. 2016, 10, 189–198. https://doi.org/10.2298/PAC1603189V
[23] Vasiljević ZZ, Dojčinović MP, Vujancević JD, Janković-Castvan I, Ognjanović M, Tadić NB, Stojadinović S, Branković GO, Nikolić MV. Photocatalytic degradation of methylene blue under natural sunlight using iron titanate nanoparticles prepared by a modified sol-gel method: Methylene blue degradation with Fe_2TiO_5. *Royal Society Open Science*. 2020, 7, 200708-200722. https://doi.org/10.1098/rsos.200708
[24] Ma Y, Zhang J, Wang Y, Chen Q, Feng Z, Sun T. Concerted catalytic and photocatalytic degradation of organic pollutants over CuS/g-C_3N_4 catalysts under light and dark conditions. *Journal of Advanced Research*. 2019, 16, 135–143. https://doi.org/10.1016/j.jare.2018.10.003

Izvod

ISPITIVANJE FOTOKATALITIČKIH OSOBINA Er^{3+} I Yb^{3+} DOPIRANOG NANOPRAHA STRONCIJUM-GADOLINIJUM-OKSIDA

Tijana Stamenković[1], Marjan Ranđelović[2], Vesna Lojpur[1]

[1]Laboratorija za atomsku fiziku, Institut za nuklearne nauke "Vinča", Institut od nacionalnog značaja za republiku Srbiju, Univerzitet u Beogradu, Beograd, Srbija
[2]Departman za hemiju, Prirodno-matematički fakultet, Univerzitet u Nišu, Niš, Srbija

(ORIGINALNI NAUČNI RAD)
UDK: 544.526.5:546.42'662
DOI: 10.5937/savteh2302004S

Cilj ovog istraživanja je da se po prvi put ispita fotokatalitička razgradnja metilen plavog na prahovima $SrGd_2O_4$ dopiranim istom koncentracijom Er^{3+} (0.5 at%) i različitim koncentracijama Yb^{3+} (1, 2.5 and 5 at%). Difrakcija rendgenskim zracima potvrdila je da uzorci kristališu u čistoj ortorombičnoj fazi. Skenirajuća elektronska mikroskopija je korišćena za ispitivanje morfologije i pokazala je da postojanje poroznih aglomerata sačinjenih od manjih čestica sferičnog oblika. Energetski disperzivna spektroskopija pokazala je prisustvo dopanata kao i uniformnu raspodelu svih elemenata u materijalu. Za izračunavanje energetskog procepa korišćena je metoda UV-VIS difuzione refleksione spektroskopije, kojom je dobijena vrednost od 4,3 eV, kao i još četri dodatne vrednosti na nižim energijama. Fotokatalitička razgradnja metilen plavog praćena je metodom UV-VIS apsorpcione spektroskopije. Dobijeni su zadovoljavajući rezultati jer je pri određenim reakcionim uslovima nakon eksperimenta u trajanju od 4 h pod dejstvom simulirane sunčeve svetlosti, potvrđena razgrađnja više od 50% od ukupne početne koncentracije boje

Ključne reči: Fotokataliza, luminescencija, retke zemlje, up-konverzija, prečišćavanje voda